Disease Extinction for Susceptible-Infected-Susceptible Models on Dynamic Graphs and Hypergraphs

Disease Extinction for Susceptible-Infected-Susceptible Models on Dynamic Graphs and Hypergraphs

Desmond John Higham[a)1, b)] and Henry-Louis de Kergorlay[1]

School of Mathematics, University of Edinburgh, Edinburgh, EH9 3FD, UK

(Dated: August 11, 2022)

We consider stochastic, individual-level susceptible-infected-susceptible models for the spread of disease, opinion, or information on dynamic graphs and hypergraphs. We set up "snaphot" models where the interactions at any time are independently and identically sampled from an underlying distribution that represents a typical scenario. In the hypergraph case this corresponds to a new Gilbert-style random hypergraph model. After justifying this modelling regime, we present useful mean field approximations. With an emphasis on the derivation of spectral conditions that determine long-time extinction, we give computational simulations and accompanying theoretical analysis for the exact models and their mean field approximations.

[a)] Corresponding author

[b)]d.j.higham@ed.ac.uk

Lead Paragraph: Humans typically interact in groups, not just in pairs. Moreover, interactions may vary over time. For these reasons, it has recently been argued that the spread of information, opinion or disease should be modelled over dynamic graphs or hypergraphs rather than a fixed graph. The use of hyperedges naturally allows for a nonlinear rate of transmission, in terms of both the group size and the number of affected group members. In the context of opinion dynamics, an individual may be affected differently if multiple members of the same group (such as a workplace or household) express a view than if the same number of contacts from different groups express that view; this is an example of a *majority effect*. Similarly, in the spread of a disease, having multiple infected contacts in the same group may lead to a different infection rate than having the same number of contacts across independent groups. In this work, we develop and study mathematical models for processes that spread over graphs and hypergraphs and we consider the case where interactions vary over time, allowing for the dynamic nature of typical encounters in, for example, offices, schools, retail and leisure outlets, public transport and entertainment events. Our overall aim in this work is to develop new mathematical models, derive useful conditions that predict when a process (such as a disease) will die out, and to test our theory with computational experiments.

I. INTRODUCTION

We consider susceptible-infected-susceptible (SIS) disease spread on a dynamically evolving graph, where the dynamic edges represent interactions between individuals in a population over time. We also consider a generalisation to the case where a disease spreads on a dynamically evolving hypergraph, where individuals interact in groups of size larger than two. Several previous works have considered SIS spreading on a dynamically evolving graph[1–12]. There, some general conditions were found which guarantee that the disease will vanish asymptotically. However, in several of those works these conditions require full exact knowledge of the dynamic graph evaluated at all times. In this work, we motivate and study the case where the dynamic graph is a sequence of i.i.d. random graphs, sampled from a static underlying expected graph, and we show how this assumption allows us to derive

simple and practical vanishing conditions. Based on a mean field approximation, we find that, in this setting, the spread of the disease on the underlying expected graph provides an accurate description of the spread of the disease on the dynamically evolving graph. We provide both numerical evidence and theoretical analysis to support this observation. We then extend our investigation to the case of a dynamically evolving hypergraph. There too we proceed via a mean field approximation, in order to derive a static hypergraph on which the spread of the disease is accurately predicted. We illustrate this approximation through numerical simulations.

The main contributions of this manuscript can be summarized as follows.

- We compare two different models of an SIS disease spreading on a (fixed or dynamic) graph, and identify the one which is more amenable for extension to the hypergraph case. In particular, we formulate and justify a new model, (18) for the spread of disease over a dynamic hypergraph.

- We propose mean field approximations (14), (17), (20) and (22) to these exact models, and illustrate their accuracy via numerical experiments. We also show that these mean field approximations provide spectral conditions which, if satisfied, guarantee the asymptotic vanishing of the disease in the population—see Theorems V.2 and V.3, and the discussion in Section VI.

- We contribute further to the theoretical analysis by estimating the difference between the infection rate of dynamic and static exact and mean field models—see Lemma V.7.

- In developing the new dynamic hypergraph model, in Section III B 1 we set up and analyse a hypergraph analogue of the classical Gilbert random graph model.

As mentioned in more detail in section II B, concepts and results in this area are relevant to many scenarios concerning the spread of information, opinion or disease; however, to be concrete, we describe the models and analysis in the language of epidemiology.

II. REVIEW OF PREVIOUS MODELS FOR THE SPREAD OF AN SIS DISEASE

A. SIS on static graphs

We first consider a population of n individuals for which we have a nonnegatively weighted, undirected graph represented by a symmetric matrix $W \in \mathbb{R}^{n\times n}$ that characterizes pairwise affinity. Here $0 \leq w_{ij} = w_{ji} \leq 1$ represents the strength of the connection between i and j, and hence will be used when we quantify the likelihood of transmission of the infection. In this graph setting, it is natural to have no self-loops; that is, $w_{ii} = 0$ for $1 \leq i \leq n$, but we note that self-loops will arise when we consider a flattening of a hypergraph—see the discussion after Definition II.3.

The SIS modelling framework places every individual in exactly one of two categories: susceptible or infected. Associated with these categories are a parameter $\beta > 0$, which quantifies the overall virulence of the disease, and a parameter $\delta > 0$, which quantifies the recovery rate. We will assume throughout that recovery of an infected individual is independent of the state of the system.

In describing various SIS models, to avoid an excess of notation we will use $p_i(t)$ to denote **both** the exact probability that individual i is infected at time t, according to a discrete or continuous time process, **and** an approximation to this quantity arising from, for example, a mean field assumption. By referring to specific models, we hope that the precise meaning of $p_i(t)$ is clear at each point in the manuscript.

In the literature there are two main approaches to modelling an SIS disease spreading on a graph. One common approach, initiated in[13], considers the parameters β and δ to be, respectively, the probability that an infected individual infects a neighbor during one unit of time, and the probability that an infected individual recovers from the disease during one unit of time. One can then derive a model as follows. Let $h > 0$ denote the time between two consecutive steps of the process. The probability $1 - p_i(t+h)$ that node i is susceptible at time $t+h$ can be expressed as the probability $h\delta p_i(t)$ that it was infected at time t but recovered at time $t+h$, plus the probability $((1-p_i(t))\prod_{j=1}^{n}(1-h\beta w_{ij}(t)p_j(t)))$ that it was susceptible at time t and did not get infected by any neighbor at time $t+h$. This gives the

following equation for all $1 \leq i \leq n$

$$1 - p_i(t+h) = h\delta p_i(t) + (1 - p_i(t) \prod_{j=1}^{n} (1 - h\beta w_{ij} p_j(t))). \tag{1}$$

In[13] spectral conditions were found which concern the asymptotic vanishing of the disease. These conditions were derived by linearizing the system, keeping only first order terms, yielding

$$p_i(t+h) = p_i(t) - h\delta p_i(t) + h\beta \sum_{j=1}^{n} w_{ij} p_j(t). \tag{2}$$

We could also move to a continuous-time setting by subtracting $p_i(t)$, dividing by h and taking the limit $h \to 0$, yielding

$$\frac{dp_i(t)}{dt} = -\delta p_i(t) + \beta \sum_{j=1}^{n} w_{ij}(t) p_j(t). \tag{3}$$

We note that (2) may be viewed as an Euler approximation to (3). Use of (1) or (2) or (3) may be regarded as a mean field approach, where we directly consider the probabilities for the nodes to be infected, rather than keeping track of the individual states of the nodes themselves.

Analysing the linearised model (2) with $h = 1$, it was shown in[13] that the disease asymptotically vanishes, that is, for all $1 \leq i \leq n$ we have $\lim_{t\to\infty} p_i(t) = 0$, if $\rho(W) < \delta/\beta$, where $\rho(\cdot)$ denotes the spectral radius. Hence, $\beta\rho(W)/\delta$ may be viewed as a graph-level analog of the classical basic reproduction number.

The authors of[14] consider an alternative approach based on Markov chains. There, we regard the state of each individual as a stochastic process $(X_i(t))_{t\geq 0}$ taking values in $\{0, 1\}$, with 0 for susceptible and 1 for infected. To this two-state valued process we associate a rate of transition matrix, where the transition rates between 0 and 1 are given as follows. If $X_i(t) = 0$, the rate of infection is given by

$$\lambda_i(X(t)) := \beta \sum_{j=1}^{n} w_{ij} X_j(t). \tag{4}$$

Here, in a very similar manner to (2), the overall chance of a new infection is taken to be linearly proportional to the number of currently infected neighbors, using the affinity weights. If $X_i(t) = 1$ the rate of recovery is given by δ. Thus, for every $1 \leq i \leq n$, the stochastic process $(X_i(t))_{t\geq 0}$ satisfies the Markov property. It is not a Markov process however, the

rates of infection being random variables. In order to use Markov theory to analyse the model further, the authors in[14] effectuate a mean field approximation by considering instead the expected infection rate $\mathbb{E}[\lambda(X_i(t))] = \beta \sum_{j=1}^n w_{ij} p_j(t)$, where $p_i(t) := \mathbb{E}[X_i(t)] = \mathbb{P}(X_i(t) = 1)$. We can now associate to the process $(X_i(t))_{t\geq 0}$ the transition rate matrix

$$Q_i(t) = \begin{pmatrix} -\beta \sum_{j=1}^n w_{ij} p_j(t) & \beta \sum_{j=1}^n w_{ij} p_j(t) \\ \delta & -\delta \end{pmatrix},$$

which makes $(X_i(t))_{t\geq 0}$ into a continuous-time Markov process. Using Markov theory for continuous-time Markov processes (e.g.,[15] (Chapter 10)), we can then deduce that $(p_i(t))$ satisfies the differential equation

$$\frac{dp_i(t)}{dt} = \beta \sum_{j=1}^n w_{ij} p_j(t)(1 - p_i(t)) - \delta p_i(t), \qquad 1 \leq i \leq n. \tag{5}$$

Let us note that (5) is very similar to the linearised model in (3), but for the $(1 - p_i(t))$ factor which, when multiplied with $\sum_{j=1}^n w_{ij} p_j(t)$, induces some second order terms. It is argued in[14] how the simplification in[13] of (1) to the linear system (2) does not provide a rigorous mean field approximation of the underlying exact processes $\{(X_i(t))_{t\geq 0}\}_{i=1}^n$. Nonetheless, we are primarily interested, in this manuscript, in the derivation of *sufficient* spectral conditions to guarantee the asymptotic vanishing of the disease. To this end, it is sufficient to consider a linear ODE which *dominates* the processes $\{(p_i(t))_{t\geq 0}\}_{i=1}^n$ in order to find sufficient spectral conditions. We note furthermore that the spectral vanishing conditions found in[13] were identical to those found in[14].

B. SIS on static hypergraphs

Another important difference to note between (1) and (5), which is of particular relevance when we wish to capture higher-order interactions between individuals, is that only the Markov chain approach (5) naturally extends to a hypergraph setting. Indeed, the rate of infection $\lambda_i(X(t))$ defined in (4) does not restrict us to pairwise interactions. The model in (1) on the other hand, via the product term in the equation, directly uses the assumption that individuals interact pairwise; an assumption that ceases to hold in the hypergraph setting. Thus previous works which studied epidemic spreading on hypergraphs (e.g.,[16–20]) consider a Markov chain approach, extending model (5). We refer to[21–23] for further details of recent work on deterministic and stochastic models for dynamics on hypergraphs.

To set up our hypergraph regime, we begin with some definitions.

Definition II.1. *Let V be a finite set, and let $E \in \mathcal{P}(V)$ be a set of subsets of V. We call the tuple (V, E) a hypergraph, where V denotes the set of nodes and E denotes the set of hyperedges.*

In particular, if all hyperedges have size two, then the hypergraph (V, E) is a standard graph with nodes V and edge set E. From now on, let $n := |V|$ and $m := |E|$.

Definition II.2. *Given a hypergraph (V, E) with $|V| = n$ and $|E| = m$, the $n \times m$ incidence matrix $\mathcal{I}$ is such that for every $(i, h) \in V \times E$, $\mathcal{I}_{ih} = 1$ if node i belongs to hyperedge h and $\mathcal{I}_{ih} = 0$ otherwise.*

Definition II.3. *Given a hypergraph (V, E) and incidence matrix $\mathcal{I}$, we define the $n \times n$ weighted clique expansion matrix $W = \mathcal{I}\mathcal{I}^T$. Here, w_{ij} records the number of hyperedges containing both nodes i and j.*

We note that in the graph case, where two nodes can be involved in at most one edge, the off-diagonal elements of the clique expansion matrix W reduce to those of the affinity matrix and the diagonal elements of W contain the node degrees—these diagonal entries may be interpreted as weighted self-loops.

In[16], the authors introduced a nonlinear function f, according to which individuals within a hyperedge may propagate the disease in a nonlinear fashion; here, the likelihood for an individual to become infected is not linearly proportional to the number of infected neighbors. Similar models were further investigated in[17,18]. The introduction of the nonlinear function f marks a significant departure from the linearity assumption that is used in typical graph-based models, and it allows us to capture features such as the *majority effect*[24] in opinion dynamics and the *viral load effect*[25] in disease spreading. We refer to[16–20] for further justification, noting that there is particular interest in the *collective suppression* case[19,20], where the function f is assumed to be concave, and the *collective contagion* case[17,18,26], where a virus spreads in a hyperedge only if at least a threshold number of individuals in the hyperedge are infected. Given any such function f, we can define the rate of infection of a node i by

$$\lambda_i(X(t)) = \beta \sum_{h \in E} \mathcal{I}_{ih} f\left(\sum_{j=1}^{n} \mathcal{I}_{jh} X_j(t) \right). \tag{6}$$

In the special case of a graph, the rate in (4) is recovered when f is the identity map. As in the graph setting, we wish to make the rates deterministic in order to apply Markov theory to this process, yielding a mean field approximation model. Two mean field approximations have been proposed and studied in[17,19,20]. In[19,20], spectral conditions were found that guarantee the asymptotic vanishing of an SIS disease spreading on a hypergraph for the different mean field models. One of the insights of[20] is that the two mean field models, while having slightly different vanishing conditions, provide very similar approximations of the exact model. Hence we shall only focus on one of the two models, the behavior of the other mean field model being conjectured to provide comparable approximations. We consider the mean field approximation obtained by replacing the infection rate (6) with a deterministic rate involving the processes given in $\{(p_i(t) := \mathbb{E}[X_i(t)] = \mathbb{P}(X_i(t) = 1))_{t\geq 0}\}_{i=1}^n$, to obtain

$$\lambda_i(X(t)) = \beta \sum_{h\in E} \mathcal{I}_{ih} f\left(\sum_{j=1}^{n} \mathcal{I}_{jh} p_j(t)\right). \tag{7}$$

This ensures that $(X_i(t))_{t\geq 0}$ is a Markov process, and as in the graph setting, we can apply Markov theory to find an ODE system for $\{(p_i(t))_{t\geq 0}\}_{i=1}^n$. We have

$$\frac{dp_i(t)}{dt} = \beta \sum_{h\in E} \mathcal{I}_{ih} f\left(\sum_{j=1}^{n} \mathcal{I}_{jh} p_j(t)\right) - \delta p_i(t), \qquad 1 \leq i \leq n. \tag{8}$$

This mean field approximation and the exact model were studied in[19] (Theorems 6.5, 8.1, 9.1), where it was found that the disease asymptotically vanishes if

$$\rho(W) < \frac{\delta}{c_f \beta}, \tag{9}$$

where $c_f > 0$ is a constant depending on the choice of f (for instance, if f is concave, $c_f := f'(0)$ is a valid choice).

We note that the internal sum in (6) runs from $j = 1$ to n, and hence includes $j = i$. Removing the $j = i$ term from this sum would not have any effect, since the infection rate for node i is only relevant when node i is uninfected; that is, $X_i(t) = 0$. However, when we move to mean field models, such as (7), removing the $j = i$ term from the sum would make a difference. In this work, in keeping with previous works, we use the full sum, and we note that computational tests suggest that specifying $j \neq i$ produces very similar results.

C. SIS on dynamic graphs

We are interested in analysing an SIS disease spread on dynamically evolving graphs and hypergraphs. Several settings for dynamic graphs have been investigated.

In[1–3,5–8,27,28], the setting consists of a dynamic graph generated from a finite number of graphs, a typical example being a periodic graph $(W(t))_{t=0}^{\infty}$, where there exists $T \in \mathbb{N}$ such that for each $k \in \mathbb{N}$, $W(k+T) = W(k)$. Then, and in other cases where the dynamic graph is generated by finitely many graphs, a spectral condition for the vanishing of the disease was given as

$$\max\{\rho(W(t)) \mid 0 \leq t \leq T\} < \frac{\delta}{\beta}.$$

In[8], the authors derive spectral conditions for the asymptotic vanishing of an SIS disease spreading on a dynamic graph under various assumptions ensuring that the dynamic graph is generated by finitely many affinity matrices $\{A(t) \mid t \in \{1, \ldots, T\}\}$. They argue that a vanishing condition can be found to be generally related to a weighted average of the spectral radii of the finitely many matrices generating the dynamic graph, the weights being proportional to the frequency of occurrence of each affinity matrix in the dynamic evolution of the graph. For instance, if the graph is periodic, cycling through each affinity matrix one by one following a fixed order, the vanishing condition they derive is given by

$$\frac{1}{T}\sum_{t=1}^{T} \rho(A(t)) < \frac{\delta}{\beta}. \tag{10}$$

We note that the authors in[8] claim that this sufficient condition can be replaced by the more compact condition

$$\rho\left(\frac{1}{T}\sum_{t=1}^{T} A(t)\right) < \frac{\delta}{\beta}. \tag{11}$$

However, since it is not true that the sum of the spectral radii is bounded above by the spectral radius of the sum, but rather that it is bounded below by the spectral radius of the sum when the matrices are Hermitian (the spectral radius then being a norm), which is the case here, we do not see how (11) arises.

From (10) we may derive a simple spectral vanishing condition that was also obtained in Theorem 2 of[6]:

$$\max\{\rho(A(t)) \mid 1 \leq t \leq T\} < \frac{\delta}{\beta}.$$

In general, we note that the vanishing conditions derived in these works require full exact knowledge of the dynamic graph, which is not a realistic assumption in many settings.

Alternatively, one can model a dynamic graph as a family of random graphs indexed by time. This is the approach considered in[4,9–11], and the relationship between discrete and continuous time network propagation is discussed in[29]. In[10], the random edges of the graphs evolve according to a Markov process. There the authors argue that the spectral vanishing condition provided by the static aggregated graph, for which the affinity matrix can be regarded as the long-time average of the affinity matrices of the random graphs, is less informative about the disease-free state of the process than another condition proved in Theorem 3.10 of[10]. This may suggest, although this was not tested by the authors of[10], that the mean field approximation induced by the static aggregated graph does not provide an accurate prediction of the exact dynamic model. This observation is an interesting contrast, but is not in contradiction with the results of this manuscript, where we show that the mean field model induced by the static underlying expected graph (which could be regarded as the analogue of the static aggregated graph) provides an accurate approximation of the exact dynamic model in a different dynamic setting (see Sections III A 2,V and Figure 1), and where the associated spectral vanishing condition is sharp.

III. SETTING AND MAIN RESULTS

A. Dynamic graphs

We define our dynamic graph with a different approach to[1–3,5–8]. Similarly to[4,9–11], we suppose that the dynamic graph is generated by random graphs. The main difference in our setting is that we assume independence of the random graphs from one time step to the other. We assume the existence of a static underlying expected graph, from which we sample at each time step, identically and independently, a new random sample matrix to represent the interactions of the individuals of the population. Intuitively, the expected graph contains information about all potential interactions a person may have over that time period (of a time step), each interaction carrying a probability weight proportional to the likelihood of this interaction occurring. To simulate a typical day (or some other relevant time period), we thus draw a random sample using the expected graph, which yields random interactions

between individuals based on the expected potential interactions which could occur. We will refer to this as a *snapshot* modelling regime for the dynamic interactions.

1. A Gilbert graph model

Let $\overline{W}$ be the affinity matrix of the static underlying expected graph. In practice, in order to build $\overline{W}$ synthetically, we will draw the entries of $\overline{W}$ at random, after which they will be treated as fixed in the model. We assume that $\overline{W}$ is a real symmetric $n \times n$ matrix, and for all $1 \leq i \leq n$, $\overline{w}_{i,j} \in [0,1]$. It is reasonable to assume that interactions are sparse in any time period; e.g., we don't expect that a person has an equal probability to visit any place in a city, but rather that they will focus a small number of places, typically in a limited neighborhood. To keep $\overline{W}$ sparse, we use a Gilbert graph model. Recall the Gilbert graph distribution $G(n,p)$, where every (undirected) edge of a random graph on n nodes, has independent probability $p \in [0,1]$ to exist[30]. We can view p as a sparsity parameter, tuned as a function of n, which allows us to control the expected degree of each node, $(n-1)p$, and to ensure the generated graph does not have too many connections, which could also make related computations too costly to perform. Let $[x_{ij}]_{i,j=1}^{n} \in [0,1]^{n^2}$, such that $x_{ij} = x_{ji}$, and let

$$\overline{w}_{ij} := \begin{cases} x_{ij} \text{ with probability } p \\ 0 \text{ with probability } 1-p. \end{cases}$$

The dynamic graph is then generated as an i.i.d. sequence of random graphs, sampled independently and identically from $\overline{W}$ as follows. Letting $\mathcal{T}' \subset \mathbb{R}_+$ be the time domain, for each $t \in \mathcal{T}'$, we sample independently $W_{ij}(t) := w_{ij}(t) \sim Bi(1, \overline{w_{ij}})$ if $i < j$, and we let $w_{ij} = w_{ji}$ if $i > j$. Informally, we toss a biased coin, with bias determined by $\overline{w_{ij}}$, to decide whether the undirected edge is created. We set $w_{ii} := 0$ for all $1 \leq i \leq n$. This gives us a dynamic graph $(W(t))_{t \in \mathcal{T}'}$. We summarize this construction by writing that each random graph was sampled independently as $W(t) \sim Bi(1, \overline{W})$. In particular, if all the entries of $\overline{W}$ are equal to 1, then $Bi(1, \overline{W}) = G(n,p)$. To each node i we associate a stochastic process $(X_i(t))_{t \in \mathcal{T}}$, where $\mathcal{T}' \subset \mathcal{T} \subset \mathbb{R}_+$. In practice $\mathcal{T}'$ is assumed to be discrete, while $\mathcal{T}$ may be discrete or continuous, but must contain $\mathcal{T}'$ as a subset. We can naturally extend the definition of W to the possibly larger time domain $\mathcal{T}$, where for all $t \in \mathcal{T}$, letting $t_0 := \max\{s \in \mathcal{T}' \mid s \leq t\}$, we let $W(t) := W(t_0)$.

2. Mean field approximations

Motivated by (4), in this dynamic setting we consider the infection rate of the process to be

$$\lambda_i(X(t)) := \beta \sum_{j=1}^{n} w_{ij}(t) X_j(t). \tag{12}$$

This rate may be approximated as before by

$$\lambda_i(X(t)) := \beta \sum_{j=1}^{n} w_{ij}(t) p_j(t), \tag{13}$$

where $p_i(t) := \mathbb{E}[X_i(t)] = \mathbb{P}(X_i(t) = 1)$, from which we derive the following ODE system to approximate the expected processes

$$\frac{dp_i(t)}{dt} = \beta(1 - p_i(t)) \sum_{j=1}^{n} w_{ij}(t) p_j(t) - \delta p_i(t). \tag{14}$$

In a discrete time setting, for instance with constant time increment equal to 1, we have the corresponding recurrence

$$p_i(t+1) = \beta(1 - p_i(t))) \sum_{j=1}^{n} w_{ij}(t) p_j(t) + (1 - \delta) p_i(t). \tag{15}$$

This last model, (15), is studied in previous work on dynamic graphs[8]. In Theorems V.2 and V.3 we show that $\mathbb{E}[\rho(W_0)] < \delta/\beta$, where $W_0 \sim Bi(1, \overline{W})$ is a random sample independent from $W(t)$, $t \geq 0$, is sufficient to ensure that $\lim_{t\to\infty} p_i(t) = 0$, almost surely (a.s.), for all $1 \leq i \leq n$ in the continuous case (14) and discrete case (15), respectively.

Another approximation of the infection rate (12), more simple than (13), is given by

$$\lambda_i(X(t)) = \beta \sum_{j=1}^{n} \overline{w_{ij}} p_i(t), \tag{16}$$

yielding the following ODE system for the associated mean field approximation in a continuous time setting

$$\frac{dp_i(t)}{dt} = \beta \sum_{j=1}^{n} \overline{w_{ij}} p_j(t)(1 - p_i(t)) - \delta p_i(t). \tag{17}$$

This approximation has the advantage that it summarizes the spread of the disease using a static graph. Such models are better understood (see Section II A), and it is known that if $\rho(\overline{W}) < \delta/\beta$, then the disease vanishes asymptotically. From a computational point of

view, running a simulation of the spread of a disease on a dynamically evolving graph can be very costly when we work at the scale of a whole city, with a very high number of nodes and interactions. The mean field approximation (17) suggests that we can obtain an accurate prediction of the disease evolution by considering the spread on a static graph, understood as the underlying expected graph of the model, where weighted edges represent the probabilities for an interaction between two individuals to occur. This mean field model thus provides us with an efficient computational method to simulate the spread of disease when the dynamically changing graph is too large to handle directly.

We compare in Section V the spectral vanishing conditions and the infection rates associated with the two mean field models (14) and (17). Under the assumption that the sparsity parameter satisfies $p = \omega(\log n/n)$, we show in Lemma V.7 that for a random sample $W_0 \sim Bi(1, \overline{W})$ we have $\rho(W_0) = \rho(\overline{W})(1 + O(1/\sqrt{pn}))$, and we show in Lemma V.6 that $S_n(i) = \mathbb{E}[S_n(i)](1 + o(1))$, where $S_n(i) := \beta \sum_{j=1} w_{ij}(t)p_j(t)$.

In Section IV, we verify numerically that the mean field model (17) induced by $\overline{W}$ provides us indeed with an accurate approximation of the behavior of the exact processes $\{(X_i(t))_{t\geq 0}\}_{i=1}^n$, thus allowing us to approximate our exact model with a disease spreading on a static graph. We do not show the other mean field approximation (14) in the figures below, since the results were visually indistinguishable from those with the more simple mean field model (17).

B. Dynamic hypergraphs

As discussed in Section II, modelling the spread of an SIS disease via a Markov process provides us with a more flexible setting, where we can consider interaction within a hyperedge, i.e., where individuals can interact in groups of size larger than two and contaminate each other in a nonlinear fashion. This more general and realistic setting has already been studied in various works[16,17,19,20,22,26,31] in the case where the higher-order structure remains static in time.

Here we investigate instead the setting where the disease spreads on a dynamically evolving hypergraph. This poses an important prior problem: which model should we use to generate a random hypergraph? Indeed, based on the various requirements one may want to impose on the hypergraph (hyperedges sizes, degree distributions, etc.), various models

can be used. Here we develop what we feel is a natural extension of the Gilbert graph model that we used in Section III A 1 to generate the random graphs.

1. A Gilbert hypergraph model

Recalling that $n \in \mathbb{N}$ represents the number of nodes (i.e., the number of individuals in the population), we now regard $m \in \mathbb{N}$ as the *targeted* number of hyperedges (i.e., the number of places where individuals can interact). We will assign nodes at random to each available hyperedge.

Definition III.1. *Let $H(n, m, q)$ denote the probability space on the set of hypergraphs of n nodes and m hyperedges, such that the incidence matrix $\mathcal{I}$ of a random hypergraph satisfies, for all $(i, h) \in \{1, \dots, n\} \times \{1, \dots, m\}$*

$$\mathcal{I}_{ih} = \begin{cases} 1 \text{ with probability } q \\ 0 \text{ with probability } 1 - q. \end{cases}$$

This definition is similar in construction to the Gilbert graph model. For instance if $n = m$, the incidence matrix of a random hypergraph in $H(n, m, q)$ corresponds to the affinity matrix of a random directed graph in $G(n, q)$. The motivation to use this model is similar to the intuition behind the model described in Section III A at the graph level. We assume that each individual has a list of potential places to visit on any given day, with a certain probability. Drawing a new random incidence matrix independently and identically at each time step simulates a typical day of people visiting places in their neighborhood.

Just as in Section III A 1, it is more realistic here to consider that the probabilities for a node to be in a hyperedge (i.e., for an individual to visit a place) vary for every pair $(i, h) \in \{1, \dots, n\} \times \{1, \dots, m\}$, so that visits can focus on a subset of locations. We also wish to keep the connections sparse. We therefore let $[x_{ih}]_{i,h=1}^{n,m} \in [0, 1]^{nm}$, q be a sparsity parameter, and set

$$\overline{\mathcal{I}}_{ih} := \begin{cases} x_{ih} \text{ with probability } q \\ 0 \text{ with probability } 1 - q. \end{cases}$$

We thus consider a weighted $n \times m$ incidence matrix $\overline{\mathcal{I}}$ which, similarly to $\overline{W}$ being the affinity matrix of the underlying expected graph in Section III A, can be thought of as the incidence

matrix of the underlying expected hypergraph from which we sample independently and identically an incidence matrix $\mathcal{I}(t)$ at every time $t \in \mathcal{T}'$.

Our sampling procedure of $(\mathcal{I}(t))_{t\in\mathcal{T}'}$ from $\overline{\mathcal{I}}$ is similar to the sampling procedure of $(W(t))_{t\in\mathcal{T}'}$ from $\overline{W}$ in Section III A 1. At each time step $t \in \mathcal{T}'$, and for each node $i \in \{1,\dots,n\}$ and hyperedge $h \in \{1,\dots,m\}$, we draw independently $\mathcal{I}_{ih}(t) \sim Bi(1,\overline{\mathcal{I}}_{ih})$. We can observe that this model does not fix a specific configuration of hyperedges of various sizes, the size of a hyperedge being unknown a priori.

As in the graph case, we then consider the Markov processes $\{(X_i(t))_{t\in\mathcal{T}}\}_{i=1}^n$, and we can naturally extend the time domain $\mathcal{T}'$ of $\mathcal{I}$ to the possibly larger domain $\mathcal{T}$ by letting for all $t \in \mathcal{T}$, $\mathcal{I}(t) := \mathcal{I}(t_0)$, where $t_0 := \max\{s \in \mathcal{T}' \mid s \leq t\}$. Following our discussion of hypergraph models in Section II, let f be a nonlinear function representing the manner in which the virus spreads in a hyperedge, and define the infection rate of a node i at time $t \in \mathcal{T}$ by

$$\lambda_i(X(t)) := \beta \sum_{h\in E} \mathcal{I}_{ih}(t) f\left(\sum_{j=1}^{n} \mathcal{I}_{jh}(t) X_j(t)\right). \tag{18}$$

Generating the random graphs in Section III A 1 as random Gilbert graphs sets all diagonal entries to 0. On the other hand, note that the sum index j spans through all values in $\{1,\dots,n\}$ including i in (18). Assuming that $f = Id$, we recover the infection rate (12) of a dynamic graph, but the induced graph here would be given by $W = \mathcal{I}\mathcal{I}^T$, hence the diagonal entries would be nonzero, indicating the degree of each node instead. As discussed at the end of section II B, we could for instance modify our infection rate (12) by restricting the inner sum to $j \in \{1,\dots,n\} \setminus \{i\}$, leading to slightly different mean field models. Such a change was found to have negligible impact on the final plots in the numerical experiments in Section IV, and would not affect the spectral vanishing conditions derived in Section V.

2. Comparison with the Gilbert graph model

Note that $H(n,m,q)$ also induces a probability space on the set of weighted graphs with n nodes. From Definition II.3, given the incidence matrix of a hypergraph $\mathcal{I}$, there corresponds a graph represented by $W := \mathcal{I}\mathcal{I}^T$, which we could call the weighted clique expansion of the

hypergraph. Every entry of this matrix is a random variable defined by

$$W_{ij} := \sum_{h=1}^{m} \mathcal{I}_{ih}\mathcal{I}_{jh}.$$

Thus the entries of the induced affinity matrix W take random values in $\{0, 1, \ldots, m\}$. Little seems to be known about how the choice of the parameters in $H(n, m, q)$ can affect properties of the induced random graph associated with W. In practice, it is important to know, for instance, how the sparsity parameter can be tuned to control the expected degree of the nodes and ensure that the graph is connected with high probability. In the case of a random Gilbert graph, it is known that connectivity of the graph holds with high probability if $p = C \log n/n$, for $C > 1$[32]. One may ask whether knowledge about the well-studied properties of random Gilbert graphs leads to results about the random Gilbert hypergraphs described above, and their induced random graph.

Let $W = \mathcal{I}\mathcal{I}^T$, where $\mathcal{I} \in H(n, m, q)$, and let $M \in G(n, p)$ be a random Gilbert graph.

By independence, we have

$$\mathbb{E}[W_{ij}] = \sum_{h=1}^{m} \mathbb{E}[\mathcal{I}_{ih}]\mathbb{E}[\mathcal{I}_{jh}] = mq^2,$$

while $\mathbb{E}[M_{ij}] = p$. Turning to the variance, we have

$$\begin{aligned}
\mathrm{Var}(W_{ij}) &= \mathbb{E}[(\sum_{h=1}^{m} \mathcal{I}_{ih}\mathcal{I}_{jh})^2] - m^2q^4 \\
&= \sum_{h=1}^{m} \mathbb{E}[\mathcal{I}_{ih}\mathcal{I}_{jh}] + \sum_{h_1 \neq h_2} \mathcal{I}_{ih_1}\mathcal{I}_{jh_1}\mathcal{I}_{ih_2}\mathcal{I}_{jh_2} - m^2q^4 \\
&= mq^2 + m(m-1)q^4 - m^2q^4 \\
&= mq^2(1-q^2),
\end{aligned}$$

while $\mathrm{Var}(M_{ij}) = p(1-p)$.

Equating the expected values, which is equivalent to equating the expected nodal degree of the two random graphs, we would choose $p := (q/m)^{1/2}$. Hence we see that for equal expected value, the variance of the entries of W is larger than the variance of the entries of M, but remains finite and contained in $[0, 1]$. We may then argue heuristically that by equating the two expected degrees of the two graph models, the variance does not differ greatly, hence the connectivity properties of the two graphs should remain similar. We have thus chosen $q := (C \log n/(mn))^{1/2}$, for some $C > 1$, to sparsify the $H(n, m, q)$-induced

graph while making sure that it remains connected with high probability. Let us emphasize that this is just a rule of thumb to derive a sensible value for the sparsity parameter q, and should not be regarded as a rigorous argument.

3. Mean field approximation

The function f in (18) represents the nonlinearity of the infection rate: specifying how the probability for a node to get infected depends on the number of infected group members. A typical choice for f is a concave function, e.g., $x \mapsto \log(1+x)$ or $x \mapsto \arctan(x)$. Another classic choice is to consider a *collective suppresion model*, where f has the form $x \mapsto c_2 \mathbb{1}(x \geq c_1)$, $c_1, c_2 > 0$.

As in Section III A, we can consider a mean field approximation with the expected processes $\{(p_i(t))_{t\in\mathcal{T}}\}_{i=1}^n := (\mathbb{E}[X_i(t)])_{t\in\mathcal{T}}$ and the deterministic infection rate at node i

$$\beta \sum_{h\in E} \mathcal{I}_{ih}(t) f\left(\sum_{j=1}^n \mathcal{I}_{jh}(t) p_j(t)\right), \tag{19}$$

yielding

$$\frac{dp_i(t)}{dt} = \beta \sum_{h\in E} \mathcal{I}_{ih}(t) f\left(\sum_{j=1}^n \mathcal{I}_{jh}(t) p_j(t)\right) - \delta p_i(t), \quad 1 \leq i \leq n. \tag{20}$$

Following Section III A, we propose to further approximate this rate of infection by substituting $\mathcal{I}_{ij}(t)$ by its expected value $\overline{\mathcal{I}_{ij}}$ for all $t \in \mathcal{T}$, thus making the infection rate completely deterministic, yielding at node i

$$\beta \sum_{h\in E} \overline{\mathcal{I}_{ih}} f\left(\sum_{j=1}^n \overline{\mathcal{I}_{jh}} p_j(t)\right), \tag{21}$$

which corresponds to the rate of infection for a disease spreading on a static hypergraph, a setting which was already studied in[16,19], yielding the ODE system

$$\frac{dp_i(t)}{dt} = \beta \sum_{h\in E} \overline{\mathcal{I}}_{ih} f\left(\sum_{j=1}^n \overline{\mathcal{I}}_{jh} p_j(t)\right) - \delta p_i(t), \quad 1 \leq i \leq n. \tag{22}$$

There, it was shown that this model satisfied a similar spectral condition for the vanishing of the disease to the graph-based model. Namely, if $f'(0)\rho(\overline{W}) < \delta/\beta$, then for all $1 \leq i \leq n$, $\lim_{t\to\infty} p_i(t) = 0$, where $\overline{W} := \overline{\mathcal{I}}\overline{\mathcal{I}}^T$. We check the accuracy of this mean field approximation in Section IV.

IV. COMPUTATIONAL EXPERIMENTS

A. Simulation algorithm for dynamic graphs

Let us first summarize our approach to simulating the exact individual-level SIS model and its mean field approximation on a dynamic graph. In the simulations, we chose $n = 600$. We used i.i.d. weights $\overline{w_{ij}}$, where $1 \leq i < j \leq n$, sampled uniformly at random in $[0, 1]$, a sparsity parameter $p := 8(\log n/n)$, and we let $(a_{ij})_{i<j}$ be i.i.d. random variables where $a_{ij} = 1$ with probability p, and $a_{ij} = 0$ otherwise. We then built the symmetric matrix $\overline{W}$, where $\overline{W}_{ij} := \overline{w_{ij}}\ a_{ij}$. The sparsity parameter p controls the amount of connectivity between the nodes of the graph. Choosing p too small will make the graph disconnected, while choosing p too large will make the graph behave like a complete graph, increasing the computational cost and failing to capture the levels of interaction that typically arise. We know from the study of random Gilbert graphs[32] that the asymptotic connectivity threshold of these random graphs occurs at $\log n/n$. Here we choose $p = 8(\log n/n)$ so that the connectivity threshold is satisfied even for small $n = 600$.

The weights of the matrix $\overline{W}$ indicate the probability for any two individuals i and j in the population to meet at any given time t. We let $\mathcal{T}' := \mathbb{N} \cap [0, T]$, where we choose the final time step to be $T := 200$, so that at every time $t \in \mathcal{T}'$, we draw an i.i.d. random sample $W(t)$ from $\overline{W}$, where $W(t)$ is symmetric, and such that for every $i < j$, $W_{ij}(t) := w_{ij}(t) = 1$ with probability $\overline{w}_{ij}$, and $w_{ij}(t) = 0$ otherwise.

We then proceed with a standard time discretization of the stochastic processes $\{(X_i(t))_{t\in[0,T]}\}_{i=1}^n$. We fix a small time step $\Delta t := 0.1$ and advance from time t to time $t + \Delta t$ at each iteration. As explained in Section II C, we extend the definition of $W := (W(t))_{t\in\mathcal{T}'}$ over this finer time partition by setting $W(t) := W(t_0)$, where $t_0 := \max\{t' \in \mathcal{T}' \mid t' \leq t\}$. We choose a vector $r \in [0, 1]^n$ of i.i.d. uniformly random values in $[0, 1]$, and for every node $i \in \{1, \ldots, n\}$,

- when $X_i(t) = 0$, we set $X_i(t + \Delta t) = 1$ if

$$r_i < 1 - \exp\left(-\lambda_i(X(t))\Delta t\right),$$

  and set $X_i(t + \Delta t) = 0$ otherwise;

- when $X_i(t) = 1$, we set $X_i(t + \Delta t) = 0$ if

$$r_i < 1 - \exp\left(-\delta\Delta t\right),$$

and set $X_i(t + \Delta t) = 1$ otherwise.

In Section II C, we proposed a mean field model (17) to approximate and simplify the above exact individual-based model. This allows us to consider the spread of a disease on the static underlying expected graph $\overline{W}$ from which we draw the random dynamic graph $W = (W(t))_{t\in\mathcal{T}}$, a setting which is well-understood and investigated in previous works (see Section II A). We simulated this system of ODE using Euler's method with time step $\Delta t = 0.1$, and tested numerically how accurately it matches the behavior of the exact process described above.

B. Simulation algorithm for dynamic hypergraphs

We simulated the exact individual-level SIS model on a dynamic hypergraph similarly, following Section III B. We chose $n = 600$ nodes, $m = 500$ hyperedges, and following the heuristic in Section II B and our choice of p in Section IV A, we chose the sparsity parameter as $q := \big(8\,\log n/(mn)\big)^{1/2}$. We then created the $n\times m$ incidence matrix $\overline{\mathcal{I}}$. As in Section IV A, we chose i.i.d. weights $\overline{x}_{ih}$ sampled uniformly at random in $[0, 1]$. Then, we let $a_{ih} := 1$ with probability q, and $a_{ih} := 0$ otherwise, and we let $\overline{\mathcal{I}_{ih}} := \overline{x}_{ih}a_{ih}$, for all $(i, h) \in \{1, \dots, n\} \times \{1, \dots, m\}$.

As in the graph setting, we then discretized the stochastic processes $\{(X_i(t))_{t\in[0,T]}\}_{i=1}^n$ with time step $\Delta t = 0.1$. The construction of the processes is the same than in Section IV A so we do not repeat it here.

The mean field approximation proposed in Section III B follows the ODE system (22) As in Section IV A, we simulated this system using Euler's method with time step $\Delta t = 0.1$.

C. Computational results

1. Dynamic graphs

In these simulations, we fixed the recovery parameter to $\delta = 1$, and varied the value of the infection parameter β, taking all the values in $\{(0.02)k \mid k \in \{0, \dots, 15\}\}$. The plots in Figure 1 show the proportion of infected individuals after a large time $T = 200$, as a function of the infection rate parameter β. The blue crosses represent the proportion of infected

individuals given by the exact model, averaged over 10 runs. The red asterisks represent the proportion of infected individuals predicted by our mean field model (17). We observe from Figure 1 that our mean field model (17) provides a very accurate approximation of the exact model. The vertical line in Figure 1 intersects the abscissa at $\beta_c := \delta/\rho(\overline{W})$. In the case where an SIS disease is spreading on a fixed graph with affinity matrix $\overline{W}$, β_c represents a threshold value, in the sense that if $\beta < \beta_c$, then the disease vanishes asymptotically from the population (e.g.,[14,33]). Here, the mean field model is defined on a fixed graph with affinity matrix $\overline{W}$, hence we can expect that the vertical line in Figure 1 serves as a threshold value for extinction of the disease, i.e., that the red asterisks will be set to 0 for $\beta < \beta_c$, but not necessarily for $\beta > \beta_c$. On the other hand, there is no such theory available to analyse SIS diseases spreading on dynamic graphs (blue crosses in Figure 1). We observe nonetheless that due to the close approximation of the exact model by the mean field model (17), β_c can also serve as a useful threshold value for extinction for the exact model spreading on the dynamic graph $(W(t))_{t\in\mathcal{T}}$.

2. Dynamic hypergraphs

We also find that the mean field model (22) provides an accurate approximation of the exact individual-based model induced by (18), as shown in Figures 2, 4, and 3. Here, as in Section IV C 1, we fixed the recovery parameter to $\delta = 1$, and varied the value of the infection parameter β, taking all the values in $\{(0.02)k \mid k \in \{0, \dots, 15\}\}$. The plots show the proportion of infected individuals as a function of β, after a large time $T = 200$. The blue crosses represent the proportion of infected individuals given by the exact model, averaged over 10 runs. The red asterisks represent the proportion of infected individuals predicted by our mean field approximation (22). For the nonlinear function f, according to which the disease spreads in a hyperedge, we used $f(x) := \log(1+x)$ (Figure 2) and $f(x) := \arctan(x)$ (Figure 3). We also tested the collective contagion model, where we apply $f(x) := x$ for edges, and for each hyperedge of size $k \geq 3$, we apply $f_k(x) := c_2^{(k)} \mathbb{1}(x \geq c_1^{(k)})$ (Figure 4). Here we chose $c_2^{(k)} = c_1^{(k)} := (k-1)/2$ for all hyperedges of size $k \geq 3$. Choosing $c_1^{(k)}$ too large, e.g., $c_1^{(k)} = k - 1$, would prevent the disease from spreading in the hyperedge even for large values of β, unless the initial proportion of infected individuals i_0 is higher than $c_1^{(k)}/k$, which would cause the plotted functions in Figure 4 to remain flat. On the

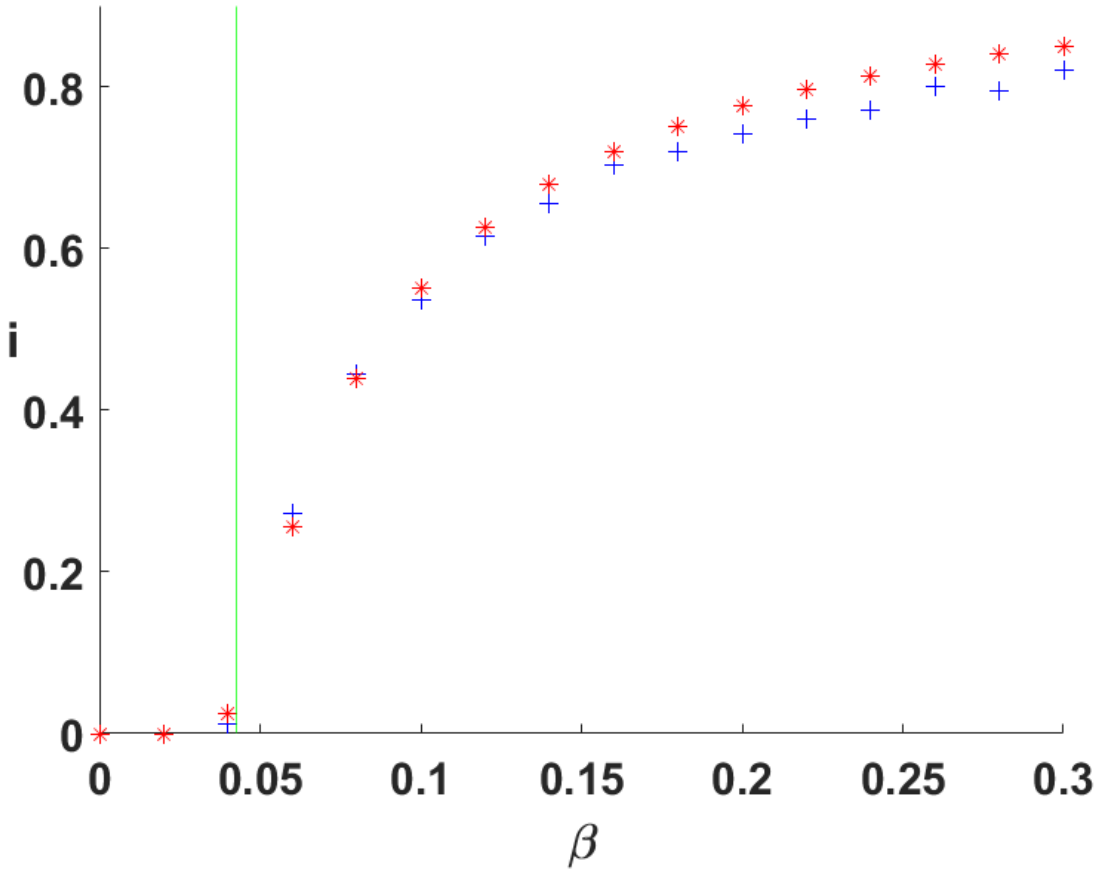

Figure 1. Dynamic snapshot graph computation. Proportion of infected individuals in the population after $T = 200$ and time step $\Delta t = 0.1$, for various values of β. Here the blue crosses represent the exact model, averaged over 10 runs, and the red asterisks represent the mean field approximation. The green vertical line represents the expected spectral threshold for extinction of the disease.

other hand, choosing $c_1^{(k)}$ too small would produce a collective contagion model similar to a linear graph-based contagion model. We can observe a discontinuity in the plots shown in Figure 4, both for the mean field approximation and the exact model, indicating that the predicted long-time proportion of infected individuals in the population is not a continuous function of the infectiousness parameter, β. This discontinuity is only observed in the case of collective contagion, and contrasts with Figures 2, 3, where the nonlinear functions representing the rate of contagiousness in the hyperedges are, respectively, $x \mapsto \log(1+x)$ and $x \mapsto \arctan(x)$, and where the plots appear to be continuous functions of β. In the case of

the collective contagion model, the nonlinear functions used to represent the contagiousness of the hyperedges are step functions, with sharply discontinuous changes of value. This implies that a small perturbation in the value of $\sum_{j=1}^{n} \mathcal{I}_{jh}(t)p_j(t)$ or $\sum_{j=1}^{n} \mathcal{I}_{jh}(t)X_j(t)$ can induce a large change of value in the resulting probability $p_j(t)$ for node j to get infected at time t. By the construction of the exact model, or by the relation describing the mean field approximation (20), we thus see that a small change in the value of β can recursively induce a large change in the value of the $p_j(t)'s$ and hence a large change in the final proportion of infected individuals. This effect is the same as the one inducing bistability and hysteresis found in[17] for the collective contagion model. The effect does not occur in Figures 2 and 3, however, since the concave functions used in the models are smooth. The spectral vanishing condition in Figure 4, represented by the green vertical line, is given by $\beta_c := \delta/\rho(W^{(2)} + \sum_{k=3}^{K}(c_2^{(k)}/c_1^{(k)})W^{(k)})$, where $W^{(k)} := \mathcal{I}^{(k)}(\mathcal{I}^{(k)})^T$, with $\mathcal{I}^{(k)}$ being the incidence matrix of the sub-hypergraph consisting only of hyperedges of size k. We can observe that this condition is less sharp than those in Figures 2 and 3, which are given by $\beta_c := \delta/f'(0)\rho(\overline{W})$. A possible explanation for this difference is that $f(x) := \log(1+x)$ and $f(x) := \arctan(x)$ are concave functions, which can be dominated by a simple linear expression: $f(x) \leq f'(0)x$. For the collective contagion analysis we used the bound $f_k(x) \leq (c_2^{(k)}/c_1^{(k)})x$, which replaces discontinuous step functions by smoother concave functions, and is likely to introduce greater inaccuracies. We leave for future work the issue of deriving better vanishing conditions for non-concave functions such as those in the collective contagion model.

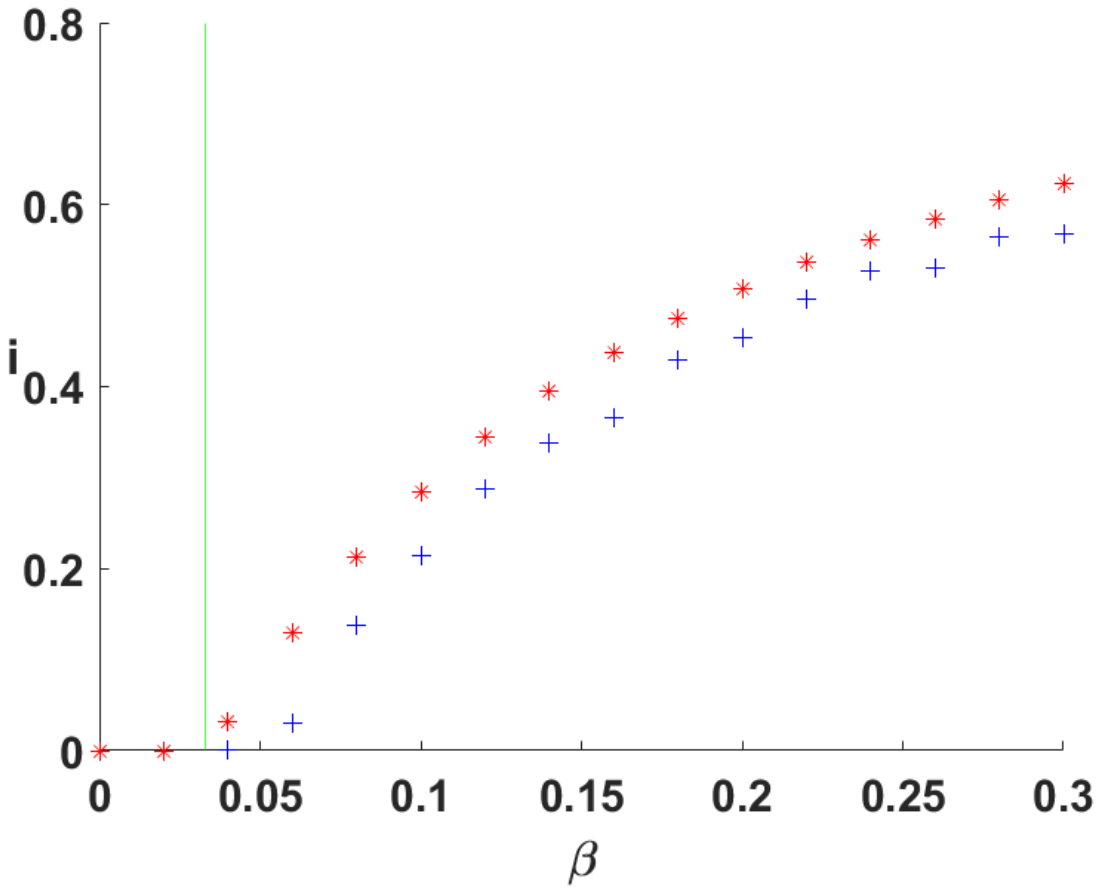

Figure 2. Dynamic snapshot hypergraph computation. Proportion of of infected individuals in the population after $T = 200$ and time step $\Delta t = 0.1$, for various values of β. Here the blue crosses represent the exact dynamic hypergraph model, where the nonlinearity function is $x \mapsto \log(1+x)$, averaged over 10 runs, and the red asterisks represent the hypergraph mean field approximation. The green vertical line represents the expected spectral threshold for extinction of the disease.

V. SUPPORTING ANALYSIS FOR THE DYNAMIC GRAPH CASE

In this section we provide theoretical analysis to support the observations made in our numerical experiments. In previous works on disease spreading on dynamic graphs ([2,7,8]), the analysis focused on the discrete-time mean field approximation (15). We analyse this model and its continuous counterpart (14) with regards to our specific assumptions on the interaction dynamics. In Section V A we derive spectral conditions which guarantee the asymptotic vanishing of the disease in the population. A corresponding result for the hypergraph case is given in Section VI.

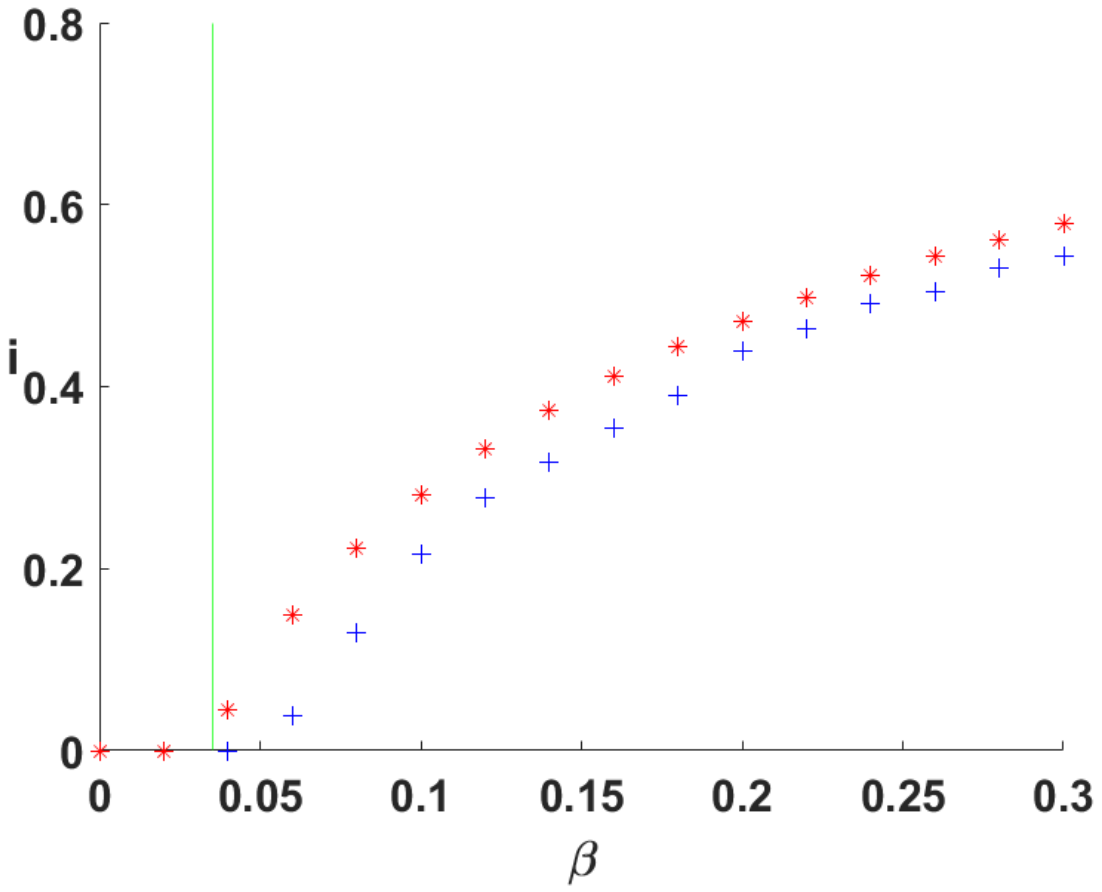

Figure 3. Dynamic snapshot hypergraph computation. Proportion of infected individuals in the population after $T = 200$ and time step $\Delta t = 0.1$, for various values of β. Here the blue crosses represent the exact dynamic hypergraph model, where the nonlinearity function is $x \mapsto \arctan(x)$, averaged over 10 runs, and the red asterisks represent the hypergraph mean field approximation. The green vertical line represents the expected spectral threshold for extinction of the disease.

In Section V B, we provide a comparison between the two mean field approximations (14) and (17), in order to justify why their plots closely match numerically. The latter model has the advantage of considering a static graph $\overline{W}$, instead of a dynamic graph $(W(t))_{t\geq 0}$, leading to a more straightforward analysis, and as we have seen in Section IV, nonetheless provides an accurate prediction of the behavior of the exact model on a dynamic graph.

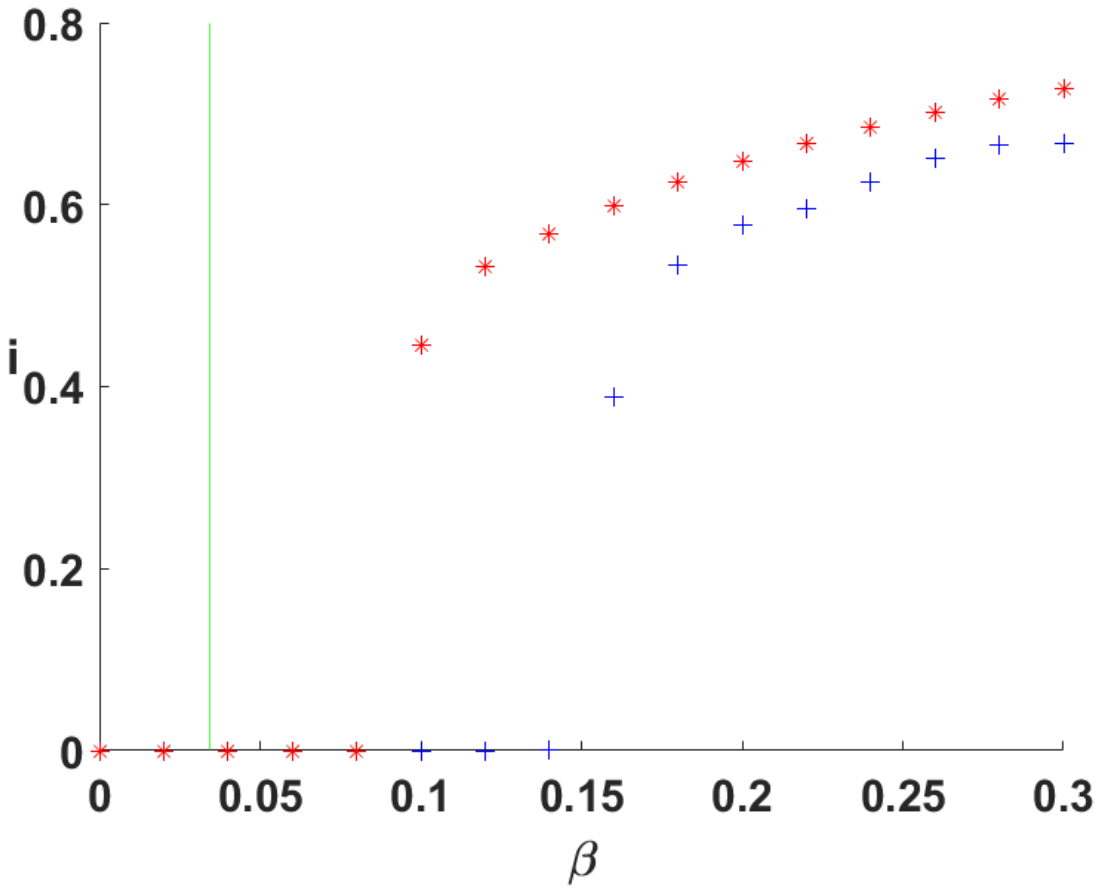

Figure 4. Dynamic snapshot hypergraph computation. Proportion of infected individuals in the population after $T = 200$ and time step $\Delta t = 0.1$, for various values of β. Here the blue crosses represent the exact dynamic hypergraph model with a collective contagion model of propagation in hyperedges, averaged over 10 runs, and the red asterisks represent the hypergraph mean field approximation. The green vertical line represents the expected spectral threshold for extinction of the disease.

A. Spectral vanishing condition

Here we derive spectral conditions which guarantee the asymptotic vanishing of the disease for the mean field approximations (14) and (15). Since we focus on deriving sufficient conditions for the vanishing of the disease, it suffices to find such conditions on a simpler system that dominates the original version. This approach was also used in previous works, as described in Section II, where for instance, the authors of[13] chose to linearize their ODE system to make it more amenable to analysis. To this end we appeal to the following result

from[20], which follows as a corollary from[34].

Corollary V.0.1 ([20]). *If, for all $1 \leq i \leq n$, we have $u_i'(t) \leq g_i(u(t))$, $y_i'(t) = g_i(y(t))$ and $u_i(0) = y_i(0)$, then $u_i(t) \leq y_i(t)$ for all $t \geq 0$.*

We also use the following lemma.

Lemma V.1. *Let $(a_T)_{T=1}^{\infty}$ be a sequence of (strictly) positive real numbers. Suppose that*

$$\lim_{T\to\infty} a_T^{1/T} < 1. \tag{23}$$

Then

$$\lim_{T\to\infty} a_T = 0. \tag{24}$$

Proof. We have

$$a_T^{1/T} = \exp\left(\frac{1}{T}\ln(a_T)\right).$$

Hence, by continuity of the exponential, condition (23) is equivalent to

$$\lim_{T\to\infty} \frac{1}{T}\ln(a_T) < -\alpha, \tag{25}$$

for some $\alpha > 0$.

If $\lim_{T\to\infty}\big|\ln(a_T)\big| < \infty$, then we would have $\lim_{T\to\infty} \frac{1}{T}\ln(a_T) = 0$, which is not the case. Hence we must have

$$\lim_{T\to\infty}\big|\ln(a_T)\big| = \infty.$$

The limit being strictly negative in (25), we can thus deduce that

$$\lim_{T\to\infty} \ln(a_T) = -\infty,$$

and hence that

$$\lim_{T\to\infty} a_T = \lim_{T\to\infty} \exp\big(\ln(a_T)\big) = 0.$$

□

Theorem V.2. *Consider the model described in (14). For all initial conditions, if $\mathbb{E}[\rho(W_0)] < \delta/\beta$, then a.s., for all $1 \leq i \leq n$, $\lim_{t\to\infty} p_i(t) = 0$, where $W_0 \sim Bi(1, \overline{W})$ is a random sample independent from $W(t)$, $t \geq 0$, and identically distributed.*

Proof. Since $(1 - p_i(t)) \leq 1$, by Corollary V.0.1, it suffices to find conditions to guarantee the asymptotic vanishing of the disease described by the following ODE system

$$\frac{dp_i(t)}{dt} = \beta \sum_{j=1}^{n} w_{ij}(t) p_j(t) - \delta p_i(t), \qquad 1 \leq i \leq n. \tag{26}$$

By assumption, $W(t)$ remains constant on every interval $t \in [kh, (k+1)h]$. On such an interval, we can thus express a solution to (26) as $P(t) = \exp((\beta W(kh) - \delta I)(t - kh))P(kh)$, where $P(t) := [p_i(t)]_{i=1}^{n}$. We thus find recursively that for all $K \in \mathbb{N}^*$,

$$P(Kh) = \prod_{k=0}^{K-1} \exp((\beta W(kh) - \delta I)h) P(0).$$

Hence a sufficient condition for the disease to vanish asymptotically is given by

$$\lim_{K \to \infty} \rho \left(\prod_{k=0}^{K-1} \exp((\beta W(kh) - \delta I)h) \right) = 0.$$

Since the spectral norm is submultiplicative, it suffices that

$$\lim_{K \to \infty} \prod_{k=0}^{K-1} \rho \left(\exp\left((\beta W(kh) - \delta I)h \right) \right) = 0,$$

and hence that

$$\lim_{K \to \infty} \prod_{k=0}^{K-1} \rho \left(\exp\left((\beta W(kh) - \delta I) \right) \right) = 0.$$

By Lemma V.1, it thus suffices that

$$\lim_{K \to \infty} \prod_{k=0}^{K-1} \rho \left(\exp(\beta W(kh) - \delta I) \right)^{1/K} < 1,$$

or equivalently, that

$$\lim_{K \to \infty} \prod_{k=0}^{K-1} \exp\left(\beta \rho(W(kh)) - \delta \right)^{1/K} < 1,$$

or equivalently, by continuity of the exponential, that

$$\lim_{K \to \infty} \beta \frac{1}{K} \sum_{k=0}^{K-1} \rho(W(kh)) - \delta < 0.$$

By the law of large numbers, we have, a.s.,

$$\lim_{K \to \infty} \frac{1}{K} \sum_{k=0}^{K-1} \rho(W(kh)) = \mathbb{E}[\rho(W_0)],$$

where $W_0 \sim Bi(1, \overline{W})$ is a random sample, and the claim follows.

□

Note that there is nothing specific about constructing W_0 as a matrix of binomial random variables in the above proof, i.e., $W_0 \sim Bi(1, \overline{W})$. A similar result holds for any other random matrix W_0 sampled with respect to a fixed expected matrix $\overline{W}$.

A similar argument yields to the same spectral vanishing condition in the discrete-time setting.

Theorem V.3. *Consider the model described in (15). For all initial conditions, if* $\mathbb{E}[\rho(W_0)] < \delta/\beta$, *then a.s., for all* $1 \leq i \leq n$, $\lim_{t\to\infty} p_i(t) = 0$, *where* $W_0 \sim Bi(1, \overline{W})$ *is a random sample independent from* $W(t)$, $t \geq 0$, *and identically distributed.*

Proof. By Corollary V.0.1, it is sufficient to find an epidemic threshold for the system of linear equations, for $1 \leq i \leq n$,

$$p_i(t+1) = (1-\delta)p_i(t) + \beta \sum_{j=1}^{n} w_{ij}(t)p_j(t), \tag{27}$$

which in matrix notation, gives

$$P(t+1) = ((1-\delta)I + \beta W(t))P(t). \tag{28}$$

We then find recursively that

$$P(t+1) = \prod_{k=t}^{0}((1-\delta)I + \beta W(k))P(0),$$

and

$$P_\infty = \lim_{t\to\infty} \prod_{k=t}^{0}((1-\delta)I + \beta W(k))P(0)$$

is well-defined and equal to 0 if

$$\rho(\lim_{t\to\infty} \prod_{k=t}^{0}((1-\delta)I + \beta W(k))) = 0.$$

By Lemma V.1, it suffices that

$$\lim_{t\to\infty} \rho\left(\prod_{k=t}^{0}((1-\delta)I + \beta W(k))\right)^{1/(t+1)} < 1.$$

The spectral norm being submultiplicative,

$$\rho\left(\prod_{k=t}^{0}((1-\delta)I + \beta W(k))\right)^{1/(t+1)} \leq \prod_{k=0}^{t}\rho((1-\delta)I + \beta W(k))^{1/(t+1)},$$

and the right hand side above, by the arithmetic-geometric mean inequality, has the bound

$$\prod_{k=0}^{t} \rho((1-\delta)I + \beta W(k))^{1/(t+1)} \leq \frac{1}{t+1} \sum_{k=0}^{t} \rho((1-\delta)I + \beta W(k))$$
$$= (1-\delta) + \beta \frac{1}{t+1} \sum_{k=0}^{t} \rho(W(k)).$$

Hence it suffices that

$$\lim_{t\to\infty} (1-\delta) + \beta \frac{1}{t+1} \sum_{k=0}^{t} \rho(W(k)) < 1,$$

and by the law of large numbers, we have a.s.

$$\lim_{t\to\infty} \frac{1}{t+1} \sum_{k=0}^{t} \rho(W(k)) = \mathbb{E}[\rho(W_0)],$$

where $W_0 \sim Bi(1, \overline{W})$ is a random sample. □

B. Comparison of the mean field approximation models

It was numerically observed that the mean field approximation model in (14) and the more simple model proposed in (17) closely matched. In this section, we compare the two mean field models by relating their respective infection rates (13) and (16), and by comparing the vanishing spectral conditions found in each case.

Let us fix $i \in \{1, \ldots, n\}$ and $t \in \mathcal{T}$. We are interested in comparing the infection rate in (13) given by $\beta \sum_{j=1}^{n} w_{ij}(t) p_j(t)$, where $\forall\ j \in \{1, \ldots, n\},\ w_{ij}(t) \sim Bi(1, \overline{w}_{ij})$, with the infection rate in (16) given by $\beta \sum_{j=1}^{n} \overline{w}_{ij} p_j(t)$. It thus suffices to estimate the right hand side in

$$\left| \sum_{j=1}^{n} (w_{ij}(t) - \overline{w}_{ij}) p_j(t) \right| \leq \left| \sum_{j=1}^{n} (w_{ij}(t) - \overline{w}_{ij}) \right|. \tag{29}$$

Definition V.4. *Let $S_n(i) := \sum_{j=1}^{n} w_{ij}$, where $w_{ij} \sim Bi(1, \overline{w_{ij}})$ independently for all $j \in \{1, \ldots, n\}$.*

Note that estimating (29) is equivalent to estimating $\left| S_n(i) - \mathbb{E}[S_n(i)] \right|$. To this end, we shall make use of Hoeffding's inequality, which states here that for all $i \in \{1, \ldots, n\}$ and all $\epsilon > 0$

$$\mathbb{P}\left(\left| S_n(i) - \mathbb{E}[S_n(i)] \right| > \epsilon \mathbb{E}[S(i)] \right) < \exp\left(-\frac{2\epsilon^2 (\mathbb{E}[S_n(i)])^2}{\sum_{i=1}^{n} \overline{w_{ij}}^2} \right) \leq \exp\left(-2\epsilon^2 \mathbb{E}[S_n(i)] \right).$$

Recall from Section II C, that we build the weights $[\overline{w}_{ij}]_{i,j=1}^n$ of the underlying static graph as follows. We let $\overline{w}_{ij} = \overline{w}_{ji} \sim x_{ij} Bi(1,p)$, where we let $[x_{ij}]_{i,j=1}^n \in [0,1]^{n^2}$ be such that $x_{ij} = x_{ji}$, $p \in [0,1]$ a sparsity parameter to be chosen, and where $\overline{w}_{ii} = 0$ for all $i,j \in \{1,\dots,n\}$.

The following lemma is a direct application of Hoeffding's inequality.

Lemma V.5. *Suppose that the sparsity parameter satisfies $p \geq \log n/n$, and that for all $i \in \{1,\dots,n\}$*

$$\sum_{j=1}^n x_{ij} = \Theta(n), \tag{30}$$

then there exists a.s. $n_0 \in \mathbb{N}$, such that for all $n \geq n_0$ and all $i \in \{1,\dots,n\}$, $\sum_{j=1}^n \overline{w}_{ij} = \Theta(pn)$.

The condition in (30) is a natural requirement that applies to most models in practice. For instance asking that the x_{ij} are uniformly bounded away from 0 for all i,j, which is natural for non-zero probability weights, implies (30). Our specific construction in Section IV, where $x_{ij} \sim \mathcal{U}[0,1]$ for all $i<j$ also satisfies this condition a.s..

Proof. By Hoeffding's inequality, for all $i \in \{1,\dots,n\}$, we have

$$\mathbb{P}\left(\left|\sum_{j=1}^n \overline{w}_{ij} - p\sum_{j=1}^n x_{ij}\right| > \epsilon p \sum_{j=1}^n x_{ij}\right) \leq \exp(-\epsilon^2 p \sum_{j=1}^n x_{ij}).$$

By the assumption in (30), there exists $C>0$ such that for all sufficiently large n and all $i \in \{1,\dots,n\}$, $\sum_{j=1}^n x_{ij} > Cn$, hence, using the assumption on p,

$$\begin{aligned}\mathbb{P}\left(\left|\sum_{j=1}^n \overline{w}_{ij} - p\sum_{j=1}^n x_{ij}\right| > \epsilon p \sum_{j=1}^n x_{ij}\right) &\leq \exp(-2\epsilon^2 pCn) \\ &\leq \exp(-2\epsilon^2 C \log n) \\ &= n^{-2\epsilon^2 C}.\end{aligned}$$

Choosing for instance $\epsilon := \sqrt{3/(2C)}$, we can conclude that

$$\mathbb{P}\left(\exists\, i \in \{1,\dots,n\}, \left|\sum_{j=1}^n \overline{w}_{ij} - p\sum_{j=1}^n x_{ij}\right| > \epsilon p \sum_{j=1}^n x_{ij}\right) \leq n^{-2},$$

hence by the Borel-Cantelli lemma, there exists a.s. $n_0 \in \mathbb{N}$, such that for all $n \geq n_0$ and all $i \in \{1, \dots, n\}$

$$\sum_{j=1}^{n} \overline{w}_{ij} = \Theta(p \sum_{j=1}^{n} x_{ij}) = \Theta(pn).$$

□

From now on, we shall assume that condition (30) holds.

Lemma V.6. *Suppose that the sparsity parameter satisfies $p = \omega(\log n/n)$, then there exists a.s. $n_0 \in \mathbb{N}$ such that for all $n \geq n_0$ and for all $i \in \{1, \dots, n\}$*

$$S_n(i) = \mathbb{E}[S_n(i)](1 + o(1)).$$

Proof. By Lemma V.5 and the choice of p, there exists α, a function of n tending to ∞ arbitrarily slowly as $n \to \infty$, such that $\min\{\mathbb{E}[S_n(i)] \mid i \in \{1, \dots, n\}\} = \alpha(n) \log(n)$. Let ϵ be a function of n, chosen such that $\epsilon(n) = o(1)$ and $\epsilon(n) = \omega(\alpha(n)^{-1/2})$. Such a choice is possible since $\alpha(n) = \omega(1)$. Using Hoeffding's inequality and our choice of ϵ, there exists $N \in \mathbb{N}$ such that for all $n \geq N$

$$\begin{aligned}
&\mathbb{P}(\exists\, i \in \{1, \dots, n\},\, \left|S_n(i) - \mathbb{E}[S_n(i)]\right| > \epsilon(n)\mathbb{E}[S_n(i)]) \\
&\qquad \leq \sum_{i=1}^{n} \mathbb{P}\left(\left|S_n(i) - \mathbb{E}[S_n(i)]\right| > \epsilon(n)\mathbb{E}[S_n(i)]\right) \\
&\qquad \leq n \exp(-2\epsilon(n)^2 \alpha(n) \log(n)) \\
&\qquad = \exp(\log(n)(1 - 2\epsilon(n)^2 \alpha(n))) \\
&\qquad \leq n^{-2},
\end{aligned}$$

and the claim follows by the Borel-Cantelli lemma. □

Recall that in Theorems V.2 and V.3 we have found the following spectral vanishing condition for the mean field approximation given by (14):

$$\mathbb{E}[\rho(W_0)] < \delta/\beta,$$

where $W_0 \sim Bi(1, \overline{W})$ is a random sample. On the other hand, the more simple mean field model proposed in (17) has the spectral vanishing condition

$$\rho(\overline{W}) < \delta/\beta.$$

We can also compare these two spectral vanishing conditions, which comes down to comparing $\mathbb{E}[\rho(W_0)]$ with $\rho(\overline{W})$.

Lemma V.7. *Suppose that the sparsity parameter of $\overline{W}$ satisfies $p \geq \log n/n$, and let $W_0 \sim Bi(1, \overline{W})$ be a random sample, we have a.s.*

$$\rho(W_0) = \rho(\overline{W})(1 + O(\frac{1}{\sqrt{pn}})).$$

Proof. Note that we can write $W_0 = \overline{W} + R$, where R is a zero mean symmetric matrix, with nonzero entries in the upper triangle that are i.i.d. and have finite variance. By Weyl's inequalities, we have in particular

$$\left|\rho(W_0) - \rho(\overline{W})\right| \leq \rho(R).$$

By the law of large numbers, we have a.s. $\rho(R) = O(\sqrt{pn})$, while by Lemma V.5 $\rho(\overline{W}) = \Theta(pn)$ a.s., from which the claimed result follows.

□

VI. ANALYSIS FOR THE DYNAMIC HYPERGRAPH CASE

The mean field approximation in (22) was noted in Section III B to be similar to the model studied in[19], where a vanishing spectral condition was shown to be

$$c_f \rho(W) < \delta/\beta,$$

where $c_f > 0$ depends on the choice of the function f.

We note furthermore that the mean field approximation in (20) can similarly be analysed. Using Corollary V.0.1, we can find a linear ODE system to dominate (20), given by

$$\frac{dp_i(t)}{dt} = c_f \beta \sum_{j=1}^{n} w_{ij}(t) p_j(t) - \delta p_i(t), \ i \in \{1, \ldots, n\}, \tag{31}$$

where $c_f > 0$ is chosen such that for all $x \geq 0$, $f(x) \leq c_f x$. As noted in[20], for the collective suppression case, where f is concave and $f(0) = 0$, we may take $c_f = f(1)$, and for a collective contagion model of the form $f(x) := c_2 \mathbf{1}(x \geq c1)$ we may take $c_f = c_2/c_1$. In (31), we have $w_{ij}(t) := \sum_{h \in E} \mathcal{I}_{ih}(t) \mathcal{I}_{jh}(t)$. We will define $W(t) := [w_{ij}(t)]_{i,j=1}^n$, and likewise $\overline{W} := \overline{\mathcal{I}} \overline{\mathcal{I}}^T$. Then we can invoke Theorem V.2, noting that the specific construction of $W_0 \sim Bi(1, \overline{W})$

there is not required, and that any other random matrix construction yields the same result. Let $\mathcal{I}_0 \sim Bi(1, \overline{\mathcal{I}})$, and let $W_0 := \mathcal{I}_0 \mathcal{I}_0^T$. By Theorem V.2, if $c_f \mathbb{E}[\rho(W_0)] < \delta/\beta$, then a.s., for all $1 \leq i \leq n$, $\lim_{t\to\infty} p_i(t) = 0$.

VII. DISCUSSION

Interactions between individuals are typically structured but dynamic—at any given time we may be likely to engage with a small subset of the population and very unlikely to engage with the rest. Our aim in this work was therefore to develop and analyze SIS spread in a snapshot-style dynamic graph framework that accounts for such interactions. Moreover, hyperedges can be used to capture the group-level interactions that take place in, for example, workplaces, schools, retail and leisure outlets, public transport and entertainment events. We therefore extended the graph-based modeling and analysis to a new dynamic hypergraph setting.

The main take-home message from our work is that a useful spectral threshold for the infection rate parameter, below which infection dies out, can be expressed in terms of an overall static expected affinity matrix (or expected clique expansion in the hypergraph case). One implication is that computationally expensive, dynamic and individual-level stochastic simulations can be replaced by cheaper deterministic mean field versions. A further implication is that in a practical scenario we can draw useful conclusions by asking individuals about their expected, or typical, interactions—this type of information is much easier to gather than more detailed microscale descriptions.

In terms of future directions, we note that our work has focused on the fundamental question of disease extinction. It would also be of interest to study more general properties of these new dynamic models; for example, along the lines developed in[16,17,21,22,26,31] for the static hypergraph case. With access to appropriate real data it would, of course, be of interest to develop methods to calibrate model parameters, compare functional forms of the infection rate, and test the predictive power of the modelling frameworks.

ACKNOWLEDGMENTS

Both authors were supported by the Engineering and Physical Sciences Research Council under grant EP/P020720/1, and DJH was also supported under grant EP/W011093/1. Code for the experiments conducted here may be found at `https://www.maths.ed.ac.uk/~dhigham/algfiles.html`.

REFERENCES

[1]B. A. Prakash, H. Tong, N. Valler, M. Faloutsos, and C. Faloutsos, "Virus propagation on time-varying networks: Theory and immunization algorithms," ECML PKDD (2010).

[2]V. S. Bokharaie, O. Mason, and F. Wirth, "Spread of epidemics in time-dependent networks," Proceedings of the 19th International Symposium on Mathematical Theory of Networks and Systems (2010).

[3]P. E. Paré, C. L. Beck, and A. Nedić, "Stability analysis and control of virus spread over time-varying networks," 54th IEEE Conference on Decision and Control , 3554 – 3559 (2015).

[4]M. Ogura and V. M. Preciado, "Stability of spreading processes over time-varying large-scale networks," IEEE Transactions on Network Science and Engineering **3**, 44 – 57 (2016).

[5]M. A. Rami, V. S. Bokharaie, O. Mason, and F. R. Wirth, "Stability criteria for SIS epidemiological models under switching policies," Discrete & Continuous Dynamical Systems - B **19**, 2865 – 2887 (2014).

[6]M. R. Sanatkar, W. N. White, B. Natarajan, C. M. Scoglio, and K. A. Garrett, "Epidemic threshold of an SIS model in dynamic switching networks," IEEE Transactions on Systems, Man, and Cybernetics: Systems **46**, 345 – 355 (2016).

[7]P. E. Paré, C. L. Beck, and A. Nedić, "Epidemic processes over time-varying networks," IEEE Transactions on Control of Network Systems **5**, 1322 – 1334 (2018).

[8]Y.-Q. Zhang, X. Li, and A. V. Vasilakos, "Spectral analysis of epidemic thresholds of temporal networks," IEEE Transactions on Cybernetics **50**, 1965 – 1977 (2020).

[9]E. Volz and L. E. Meyer, "Epidemic threshold in dynamic contact networks," The Royal Society Interface **6** (2009).

[10]Y. Schwarzkopf, A. Rákos, and D. Mukamel, "Epidemics spreading in evolving networks," Phys. Rev. E **82** (2010).

[11]M. Doostmohammadian, H. R. Rabiee, and U. A. Khan, "Centrality-based epidemic control in complex social networks," Social Network Analysis and Mining **10** (2020).

[12]S. Chowdhary, A. Kumar, G. Cencetti, I. Iacopini, and F. Battiston, "Simplicial contagion in temporal higher-order networks," Journal of Physics: Complexity **2**, 035019 (2021).

[13]Y. Wang, D. Chakrabarti, C. Wang, and C. Faloutsos, "Epidemic spreading in real networks: an eigenvalue point of view," Proceedings 22nd International Symposium on Reliable Distributed Systems (2003).

[14]P. V. Mieghem, J. Omic, and R. Kooij, "Virus spread in networks," IEEE Transactions on Networking **17** (2009).

[15]P. van Mieghem, *Performance Analysis of Communications Networks and Systems* (Cambridge University Press, Cambridge, 2010).

[16]A. Bodó, G. Katona, and P. Simon, "SIS epidemic propagation on hypergraphs," Bulletin of Mathematical Biology **78**, 713–735 (2016).

[17]G. F. de Arruda, G. Petri, and Y. Moreno, "Social contagion models on hypergraphs," Phys. Rev. Res. **2** (2020).

[18]N. W. Landry and J. G. Restrepo, "The effect of heterogeneity on hypergraph contagion models," Chaos **30** (2020).

[19]D. J. Higham and H.-L. de Kergorlay, "Epidemics on hypergraphs: Spectral thresholds for extinction," Proceedings of the Royal Society, Series A (2021).

[20]D. J. Higham and H.-L. de Kergorlay, "Mean field analysis of hypergraph contagion models," arXiv:2108.05451 (2021).

[21]F. Battiston, E. Amico, A. Barrat, G. Bianconi, G. Ferraz de Arruda, B. Franceschiello, I. Iacopini, S. Kéfi, V. Latora, Y. Moreno, M. M. Murray, T. P. Peixoto, F. Vaccarino, and G. Petri, "The physics of higher-order interactions in complex systems," Nature Physics **17**, 1093–1098 (2021).

[22]F. Battiston, G. Cencetti, I. Iacopini, V. Latora, M. Lucas, A. Patania, J.-G. Young, and G. Petri, "Networks beyond pairwise interactions: Structure and dynamics," Physics Reports **874**, 1–92 (2020).

[23]S. Majhi, M. Perc, and D. Ghosh, "Dynamics on higher-order networks: A review," Journal of the Royal Society Interface **19**, 20220043 (2022).

[24]A. Koriat, S. Adiv-Mashinsky, M. Undorf, and N. Schwarz, "The prototypical majority effect under social influence," Personality and Social Psychology Bulletin **44**, 670–683 (2018).

[25]M.-A. de La Vega, G. Caleo, J. Audet, X. Qiu, R. A. Kozak, J. I. Brooks, S. Kern, A. Wolz, A. Sprecher, J. Greig, K. Lokuge, D. K. Kargbo, B. Kargbo, A. D. Caro, A. Grolla, D. Kobasa, J. E. Strong, G. Ippolito, M. V. Herp, and G. P. Kobinger, "Ebola viral load at diagnosis associates with patient outcome and outbreak evolution," The Journal of Clinical Investigation **125**, 4421–4428 (2015).

[26]I. Iacoponi, G. Petri, A. Barrat, and V. Latora, "Simplicial models of social contagion," Nature Communications **10** (2019).

[27]E. Valdano, L. Ferreri, C. Poletto, and V. Colizza, "Analytical computation of the epidemic threshold on temporal networks," Physical Review X **5**, 021005 (2015).

[28]L. Neuhäuser, R. Lambiotte, and M. Schaub, "Consensus dynamics on temporal hypergraphs," Physical Review E **104**, 064305 (2021).

[29]E. Valdano, M. Fiorentin, C. Poletto, and V. Colizza, "Epidemic threshold in continuous-time evolving networks," Physical Review Letters **120**, 068302 (2018).

[30]E. N. Gilbert, "Random graphs," The Annals of Mathematical Statistics **30**, 1141–1144 (1959).

[31]U. Alvarez-Rodriguez, F. Battiston, G. F. de Arruda, Y. Moreno, M. Perc, and V. Latora, "Evolutionary dynamics of higher-order interactions in social networks," Nat. Hum. Behav. (2021).

[32]A. Frieze and M. Karoński, *Introduction to Random Graphs* (Cambridge University Press, Cambridge, UK, 2015).

[33]A. Ganesh, L. Massoulié, and D. Towsley, "The effect of network topology on the spread of epidemics," Proceedings - IEEE INFOCOM **2**, 1455–1466 (2005).

[34]M. Petrovitch, "Sur une manière d'étendre le théorème de la moyenne aux équations différentielles de premier ordre," Mathematische Annalen **54**, 417–436 (1901).